Coupled-spin–mobile-hole model for high-T_c superconducting oxides

E. Y. Loh, Jr., T. Martin, P. Prelovsek,* and D. K. Campbell
Center for Nonlinear Studies, Los Alamos National Laboratory, Los Alamos, New Mexico 87545
(Received 23 December 1987)

A model representing a system of coupled localized spins and mobile holes and relevant to superconducting oxides is analyzed by performing both exact diagonalizations on small systems and variational calculations. Ground-state expectation values, susceptibilities, optical conductivity, and pairing correlations are calculated for systems with up to six unit cells arranged on a ring or representing a square lattice. With increasing spin–mobile-hole coupling, our results show a transition to a regime of mobile singlets and short-range magnetic correlations. On the square lattice, the interaction weakly enhances the d-wave pairing, but suppresses s-wave and extended s^*-wave correlations.

I. INTRODUCTION

In the recent search for microscopic models for the high-T_c superconducting (SC) copper oxides, many variants of the Hubbard model have been studied. Based on the underlying idea that a purely excitonic mechanism[1] might explain the onset of the SC state at high temperatures, single-band Hubbard models were first investigated;[2–4] these models take into account effectively only a single orbital per CuO_2 unit cell in the oxide layers. Results on possible electron-pairing mechanisms in these models are still controversial,[2–6] and more accurate (numerical) many-body studies on larger-sized systems and at lower temperatures will be required to resolve this controversy.

Several authors have recently considered a more realistic two-band Hubbard model,[7–12] which explicitly includes both Cu and O orbitals in the unit cell. One clear motivation for studying this more-complicated situation is that for parameter regimes relevant to the SC copper oxides the results for the two-band model cannot be mapped (at least not in a straightforward way) onto a single-band model. Further, it appears that in doping the reference substance—which for definiteness we consider to be La_2O_4—the resulting holes seem predominantly to occupy p orbitals on O sites.[12]

To date, most studies of the two-band Hubbard model have been devoted to the search for local (real-space) pairing of holes on O sites in the presence of the antiferromagnetically (AFM) ordered (or correlated) spins on Cu sites. An attraction due to the spin exchange between two holes on neighboring O sites has been claimed in Refs. 7 and 9; however, this seems to be overcome by the repulsion due to the loss of the kinetic energy. Hirsch[8] argues in favor of the hole-hole attraction due to intermediate broken (AFM) bonds; the validity of this argument remains unclear, for it would seem to apply well to a single-band Hubbard model.

In a previous paper,[10] one of the present authors derived from an initial two-band Hubbard model a reduced Hamiltonian describing a coupled system of localized spins on Cu sites and mobile holes on O sites. The simplification, which is based on the elimination of the strong on-site (Cu) Coulomb repulsion from the problem, has the conceptual advantage that, for intermediate spin-hole interaction, it focuses *directly* on the coupling of two relevant degrees of freedom—namely, the mobile carriers on the O sites and magnetic fluctuations mainly due to spin on Cu sites—currently thought to be relevant in SC oxides. An analogous separation has proved to be a difficult problem in a single-band Hubbard model. In our previous paper[10] the simplified model was studied perturbatively for a low concentration of holes in the AFM phase. The results showed a substantial enhancement of the hole effective mass and a strong sensitivity of the AFM order to doping. In addition, the hole-hole interaction through the AFM magnons was shown[10] to be ineffective for producing SC pairing, at least in the weak-coupling and the very-low-doping regimes.

Recently, Zhang and Rice[11] used similar intermediate steps, taking into account also more explicitly the phases of p and d orbitals, to map the two-band Hubbard model onto an effective single-band model for a motion of local singlets, formed by mobile holes and Cu spins. The qualitative difference from our approach[10] stems mainly from the larger spin-hole interaction assumed in Ref. 11; in contrast, we are able to study a range of interaction strengths.

In the present article we study the coupled spin-hole model via exact diagonalization of small systems and a variational ansatz. Our aim is to provide results valid *beyond* the perturbative coupling regime and, in addition, beyond the low-doping regime in which AFM ordering holds. Such nonperturbative, true many-body results are essential to test the validity (or failure) of the physical intuition supporting the basic model.

We have organized our presentation in the following manner. First, in Sec. II we present the coupled spin–mobile-hole model and review briefly its derivation. In Sec. III we treat a one-dimensional version of this model in detail. We present results for static and dynamic quantities, including spin correlations, magnon characteristic frequencies, and the optical conductivity. Experimentally, this last observable is particularly important, for it gives direct evidence concerning the masses and internal structure of the mobile quasiparticles in the doped, in-

teracting system. The early experiments[13–15] on polycrystalline samples suggested that the low-frequency optical conductivity was not Drude-like, but rather was dominated by a peak at $\simeq 0.5$ eV. Theoretical proposals have been advanced interpreting this mode in terms of an excitonic mechanism[16] or alternatively in terms of strong polaronic effects,[17] which are reflected in a very large enhancement of the effect mass and consequently small weight of the Drude peak. More recent data[18] on single crystals of Y-Ba-Cu-O *do* show a normal, Drude-like optical structure, suggesting that the earlier results were not intrinsic to the materials but were due to the unoriented, polycrystalline nature of the samples. Our study suggests that within the spin–mobile-hole models the effective mass of the quasiparticles, although enhanced, remains of the order of the "bare" hole mass; hence, consistent with the single-crystal data,[18] we expect that a Drude-like structure should be observed in experiments measuring the intrinsic optical absorption. In Sec. IV a variational approach, essentially an extension of the conventional classical spin approximation[19] in the magnetic polaron problem,[20] is compared with our exact results. In Sec. V results for a small two-dimensional "square" lattice, including the analysis of the SC pairing, are discussed.

II. THE COUPLED-SPIN–MOBILE-HOLE MODEL

In our previous paper[10] the two-band Hubbard model for electrons within CuO_2 layers (see Fig. 1), as proposed by Emery,[7] was reduced to a model of coupled localized spins on Cu sites and mobile holes, predominantly on O sites. In terms of the parameters of the original model the $p(O)d(Cu)$ hybridization energy t_0, the difference of hole energy on the O and Cu sites $\Delta\varepsilon=\varepsilon_0-\varepsilon_{Cu}$, and the on-site Coulomb repulsions U_{Cu}, U_O, the underlying assumption is that $\Delta\varepsilon > t_0$ and $U_{Cu} \gg t_0$. The resulting two-orbital model is expressed in terms of the creation (annihilation) operators for holes $c_{ls}^\dagger$ (c_{ls}), occupying p_x (p_y) orbitals on O sites, and spins $\mathbf{S}_i$ ($S=\frac{1}{2}$ since we use units with $\hbar=1$) on Cu sites,

$$H=-t\sum_i p_i+\sum_i (V_1\mathbf{q}_i+V_2\eta_i)\cdot\mathbf{S}_i+J\sum_{\langle i,j\rangle}\mathbf{S}_i\cdot\mathbf{S}_j\,, \tag{1}$$

where $\langle i,j\rangle$ denotes nearest-neighbor pairs and p_i, $\mathbf{q}_i$, and η_i are related to hole operators within a CuO_4 group around the given ith Cu site,

$$p_i=\sum_{\substack{l,m,s\\ l\neq m\in i}} c_{ls}^\dagger c_{ms},\quad \mathbf{q}_i=\tfrac{1}{2}\sum_{\substack{l,m,s,s'\\ l\neq m}}\sigma_{ss'}c_{ls}^\dagger c_{ms'}\,,$$
$$\eta_i=\tfrac{1}{2}\sum_{\substack{l,s,s'\\ l\in i}}\sigma_{ss'}c_{ls}^\dagger c_{ls'}\,. \tag{2}$$

The first term in (1) represents effective free-hole motion, whereas the last one is the exchange coupling between Cu spins. The interaction term contains a direct exchange (V_1 term) of O holes and Cu spins and the exchange through the hole hopping (V_2 term). Note that since in Eqs. (1) and (2) we do not consider explicitly the phases of the p and d orbitals, our model is written for effective s-like orbitals. Zhang and Rice[11] have recently pointed out that a proper treatment of this phase problem could lead to quantitative differences. It should be stressed that in the Hamiltonian of Eq. (1) the reference substance—e.g., La_2CuO_4—is a magnetic insulator described entirely by a Heisenberg Hamiltonian for spins on the Cu sites. The $c_l^\dagger$ describe holes created *relative* to this (half-filled) reference substance, and only these mobile holes, introduced into real superconducting materials by doping the reference substance, can lead to a normal-state conductivity and finally (possibly) to superconductivity.

To lowest order in t_0, parameters in (1) and (2) are related to those in the Hubbard model as follows: $2t=t_1+t_2$, $V_1/2=t_2-t_1$, $V_2/2=t_2+t_3$, where $t_1=t_0^2/\Delta\varepsilon$, $t_2=t_0^2/(U_{Cu}-\Delta\varepsilon)$, and $t_3=t_0^2/(U_0+\Delta\varepsilon)$. It follows from these relations that t, V_1, and V_2 are of the same order magnitude, while $J\propto t_0^4/\Delta\varepsilon^2 U_{Cu}\ll t$. Although the derivation is systematic only for small t_0, the model defined by (1) and (2) can be regarded as the simplest prototype containing the relevant invariants.

A further simplification is possible if $V_1, V_2 < t$. Then a single symmetrized hole orbital (out of two orbitals on O sites per cell) per CuO_4 can be used, and the model can be written as

$$H=-t\sum_{\langle i,j\rangle,s}(c_{is}^\dagger c_{js}+c_{js}^\dagger c_{is})+V\sum_i \mathbf{s}_i\cdot\mathbf{S}_i+j\sum_{\langle i,j\rangle}\mathbf{S}_i\cdot\mathbf{S}_j\,, \tag{3}$$

where $c_{is}^\dagger$ (c_{is}) now refer to a symmetrized hole orbital within the ith unit cell and $\mathbf{s}_i$ is the corresponding local spin operator for mobile holes. In a square lattice the relation between coupling constants is $V=6V_1+2V_2$. Although for larger V_1, V_2 the simplification to Eq. (3) cannot be justified adequately, we still believe that this reduced model contains most of the relevant physics: namely, it leads for large couplings to the formation of localized singlets (see also Ref. 11), composed by Cu spins and mobile-hole spins. As we will discuss, the internal structure of these singlets depends on the particular model.

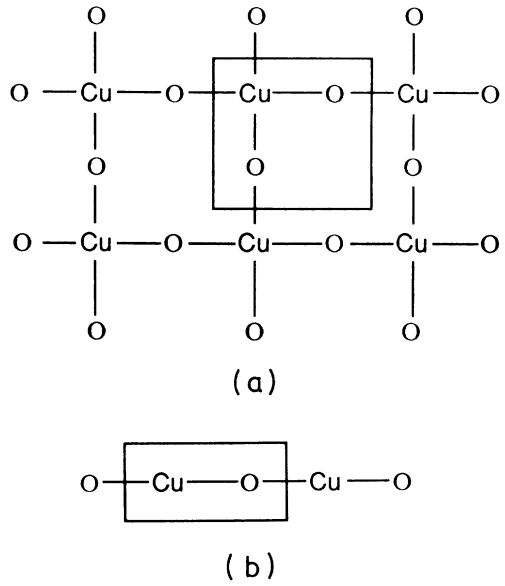

FIG. 1. Copper oxide structures with one Cu per unit cell. (a) CuO_2 plane. (b) $(CuO)_x$ chain.

For a numerical study, the reduction of the number of fermion sites allows a substantial increase of the number of unit cells in the system. Hence, for two-dimensional systems we will consider only the simplified model (3), while for rings we also present results for the model (1). Note that the model (3) is effectively a Kondo-lattice Hamiltonian, but we are interested in the limit of a large number of spins and a small number of mobile holes.

Since the number of states grows exponentially with system size, our exact diagonalizations of the spin-hole model must focus on fairly small systems. Thus we have focused on four and six unit-cell systems with at most two mobile holes. Further, for simplicity, we have used an algorithm that restricts only $S^z_{\rm tot}$ and $\mathbf{S}_{\rm tot}\cdot\mathbf{S}_{\rm tot}$. There are a few advantages in first solving a $d=1$ model, i.e., the problem of CuO chains. First, the consideration of rings (chains with periodic boundary conditions) permits a comparison between models (1) and (3). Also, the larger linear dimensions permit a more-accurate evaluation of the optical conductivity, since it is a $q\rightarrow 0$ property.

III. NUMERICAL RESULTS FOR RINGS

Let us consider the model (3) on a ring of N cells. The conserved quantities in this case are the number of holes n_h, the total z spin $S^z_{\rm tot}$ of the system, the total spin squared $\mathbf{S}_{\rm tot}\cdot\mathbf{S}_{\rm tot}$, and the quasimomentum q_0 (due to the translational invariance). We use only the first two symmetries to reduce the number of basis states. For the largest case considered, $N=6$ and $n_h=2$. For $S^z_{\rm tot}=0$, either both holes have spin up [$\binom{6}{2}$ such states] and four of the six localized spins are down [$\binom{6}{4}$ such states], one hole is up and the other is down [$\binom{6}{1}^2$ such states] and three of the six localized spins are down [$\binom{6}{3}$ such states], or both holes have spin down [$\binom{6}{2}$ again] and two localized spins are down [$\binom{6}{2}$]. Our largest matrix, then, has $\binom{6}{2}\binom{6}{4}+\binom{6}{1}^2\binom{6}{3}+\binom{6}{2}\binom{6}{2}=1170$ states.

Using the calculated exact wave functions for the ground state $|\psi_0\rangle$ and excited states $|\psi_m\rangle$, we evaluate the following observable quantities.

(a) The local spin-hole spin correlation function, given by

$$\zeta=-\sum_i\langle\psi_0|\mathbf{s}_i\cdot\mathbf{S}_i|\psi_0\rangle/n_h\,. \tag{4}$$

This quantity indicates the extent of the formation of local singlets. Note that $E_{\rm int}=-\zeta n_h V$.

(b) The total spin correlations and static susceptibilities:

$$C(q)=\langle\psi_0|S^z_{\rm tot}(q)S^z_{\rm tot}(-q)|\psi_0\rangle\,, \tag{5}$$

$$\chi(q)=2\sum_{m\neq 0}|\langle\psi_0|S^z_{\rm tot}(q)|\psi_m\rangle|^2/(E_m-E_0)\,, \tag{6}$$

where

$$\mathbf{S}_{\rm tot}(q)=\frac{1}{\sqrt{N}}\sum_i e^{i\mathbf{q}\cdot\mathbf{R}_i}(\mathbf{S}_i+\mathbf{s}_i)\,. \tag{7}$$

From the dynamical susceptibilities, we can evaluate frequency moments of magnetic excitations; e.g., the first frequency moment is given by $\bar{\omega}(q)=C(q)/\chi(q)$.

(c) In order to study optical-absorption properties of the system, we define the ac conductivity for a finite wave vector q,

$$\mathrm{Re}\sigma(q,\omega)=Na_0\sum_m\frac{1}{\omega}|\langle\psi_0|j_q|\psi_m\rangle|^2\delta(\omega-E_m+E_0)\,, \tag{8}$$

where a_0 is the lattice constant and the current operator is given by

$$j_q=\frac{ie_0t}{N}\sum_{i,s}(c^\dagger_{is}c_{i+1,s}-c^\dagger_{i+1,s}c_{is})e^{iqR_i}\,. \tag{9}$$

It can be shown that for $q\neq 0$ the conductivity satisfies the sum rule

$$\int_{-\infty}^{\infty}\sigma(\varepsilon,\omega)d\omega=\frac{e_0^2a_0t}{N}\sum_{i,s}\langle\psi_0|c^\dagger_{i+1,s}c_{is}+c^\dagger_{is}c_{i+1,s}|\psi_0\rangle$$
$$=-\frac{e_0^2a_0}{N}E_{\rm kin}\,, \tag{10}$$

relating the integrated conductivity to the ground-state energy. In the case of a parabolic band the sum rule reduces to a well-known expression, since then $E_{\rm kin}=-n_h/m^*a_0^2$, where m^* is the effective band mass of holes. For periodic boundary conditions $\sigma(q=0,\omega)$ does not directly satisfy Eq. (10); hence, we use the lowest nonzero $q=(2\pi/Na_0)$ allowed in the system for our analysis.

(d) The possibility of SC pairing can be monitored by the behavior of the pair correlation functions

$$Z_{rr'}=\langle\psi_0|\Delta^\dagger_r\Delta_{r'}|\psi_0\rangle\,, \tag{11}$$

where on the ring we consider s-wave, extended s^*-wave, and p-wave operators, defined respectively by

$$\Delta_s=\sum_i c_{i\uparrow}c_{i\downarrow},\quad \Delta_{s^*}=\sum_i c_{i\uparrow}(c_{i-1\downarrow}+c_{i+1\downarrow})\,,$$
$$\Delta_p=2\sum_i c_{i\uparrow}c_{i+1\uparrow}\,. \tag{12}$$

A tendency towards real-space pairing would also show up in the hole-density correlation functions

$$g_{ij}=\langle\psi_0|n_in_j|\psi_0\rangle\,, \tag{13}$$

where $n_i=\sum_s c^\dagger_{is}c_{is}$.

In the following we present results for $N=6$ with $n_h=1$ and 2 and $S_{\rm tot}\neq 0$. For comparison, we also present $N=4$, $n_h=1$ and 2 cases. Apart from expected differences due to the different effective doping levels, in most quantities there is no crucial difference between $N=4$ and $N=6$ results. For the $N=6$ system, however, the ground state becomes degenerate for a certain range of J for large V/t. This degeneracy is due to the appearance of a stable inhomogeneous $q_0\neq 0$ state, which can be interpreted as an analog in the present case of the Peierls instability that occurs at finite coupling in finite-size electron-phonon systems. For all cases with $n_h=2$, the total singlet state is lower in energy than $S_{\rm tot}\neq 0$ states. There are, however, a few subtle differences between $n_h=1$ and $n_h=2$ results, especially in the magnetic properties within the intermediate-coupling regime; as we shall see, these can be partly attributed to nonzero $S_{\rm tot}$ ($=\frac{1}{2}$ for $n_h=1$).

In Figs. 2(a) and 2(b) we plot the results for local spin correlations ζ as a function of V/t for several J/t. It should be noted that the relevant values for J, as observed in the CuO_2 layers (e.g., by neutron scattering[21] in La_2CuO_4), seem to be in the range $J/t=0.1$–0.2. From Fig. 2(a) it follows that ζ increases nearly linearly for small V/t and then jumps to a more-correlated state for $V>V^*(J)$. At large $V\to\infty$, ζ approaches the maximum value $\zeta=\frac{3}{4}$, showing that the $\mathbf{s}_i$ and $\mathbf{S}_i$ form local singlets. A linear variation of ζ for small V and low hole concentration was obtained analytically for a square lattice in Ref. 10 using the expansion in the magnons within the AFM ground state. Note that $E_{\rm int}/n_h=-\zeta V$ can be interpreted as the main contribution to the magnetic polaron binding energy. The same perturbation procedure cannot be directly applied to the $d=1$ problem due to the absence of AFM long-range order for $V=0$. Nevertheless, the qualitative behavior seems to remain the same, e.g., for small V, ζ is nearly independent of J.

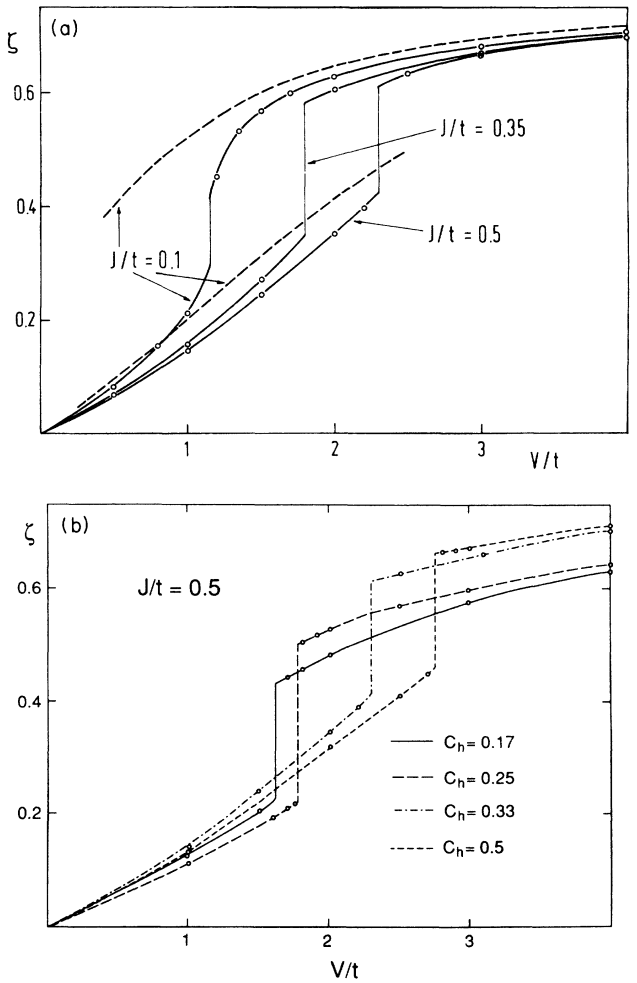

FIG. 2. Local spin correlation ζ as a function of V/t for (a) different J/t at fixed hole concentration $c_h=\frac{1}{3}$ ($N=6$ sites, $n_h=2$ holes), and (b) at fixed $J/t=0.5$ for various c_h (combinations of $N=4,6$ and $n_h=1,2$). In (a) dashed curves denote analytical results, Eqs. (20)–(22), following from the variational approach.

The transition at $V^*(J)$, which is clearly discontinuous for $J/t>0.1$, shows up in all quantities. The state at $V>V^*$ is characterized by well-formed local singlets, but also by a change in the short-range order of S_i spins. Whereas for $V<V^*$ short-range correlations $C_1=\langle\mathbf{S}_i\cdot\mathbf{S}_{i+1}\rangle$ are AFM or even more singletlike, e.g., $C_1=-0.46$, they are strongly reduced for $V>V^*$ (and $J/t=0.35$, 0.5) and even become weakly *ferro*magnetic (FM), i.e., $C_1>J/t=0.1$. These qualitative changes, at least for $J/t=0.1$, are well described by the variational ansatz as described in Sec. IV. We note also that the ground states for $J/t=0.35$, 0.5 are inhomogeneous, i.e., $q_0\neq 0$, and hence degenerate.

Figure 2(b) shows results for ζ as calculated for different concentrations of holes, as simulated by choosing different combinations of system sizes $N=4,6$ and holes $n_h=1,2$. The transition value $V^*(J)$ decreases with decreasing concentration $c_h=n_h/N$. V^*, however, seems to approach a finite value at $c_h\to 0$; in Sec. IV we will argue that this is natural, since the transition is "local."

Results for spin correlations, as defined by Eq. (5), are presented in Fig. 3. For both $J/t=0.1$ and 0.5, the correlations have a clear maximum at $q_m=\pi/a_0$ for $V<V^*$. The abrupt change at $V=V^*$ moves the maximum to $q_m\neq\pi/a_0$; in particular, in our small system we find $q_m=\pi/3a_0$ for $J/t=0.1$ and $q_m=2\pi/3a_0$ for $J/t=0.5$. These different q_m can be explained by noting that smaller J allows for more FM local correlations which induce smaller q_m. The same is not the case for larger J due to the loss of the exchange energy of Cu spins. The abruptness of the transition at $V=V^*$ is also connected with the result that for $V>V^*$ the emerging local singlets (for the case $n_h=2$) occupy most distant possible sites; this is clearly indicated by the hole-density correlations, i.e., the large values of $g_{i,i+N/2}\gg g_{i,i+1}$. Thus, in the $N=6$ system, $g_{i,j\neq i}=0.055$ for $V=0$, while $g_{i,i+1}=0.03$ and $g_{i,i+3}=0.1$ for $V=1.5$ and $J/t=0.1$. When formed, these singlets effectively break the ring into weakly communicating parts; obviously this is an effect particular to $d=1$. It is reflected also in a rather peculiar behavior of magnon modes $\omega(q)$ for $V>V^*$, as shown in Fig. 4. For

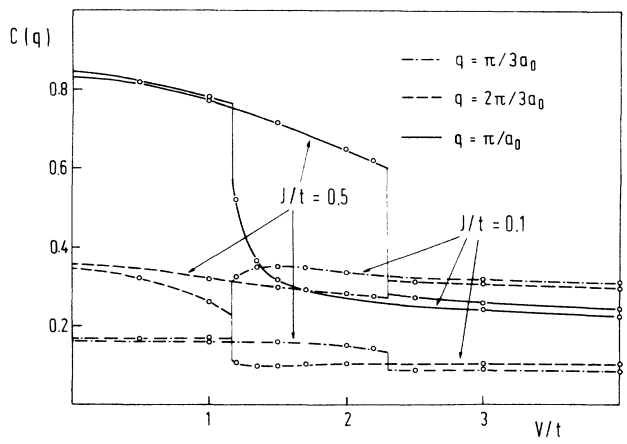

FIG. 3. Total spin correlation $C(q)$ as a function of V/t for a $d=1$ ring with $N=6$ and $n_h=2$.

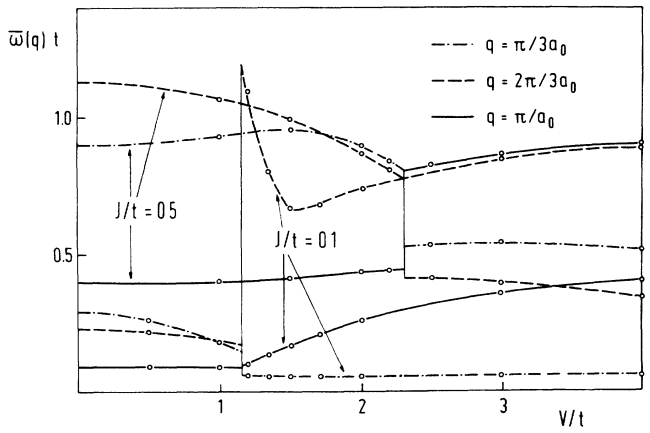

FIG. 4. Spin-fluctuation frequencies $\bar{\omega}(q)$ for a $d=1$ ring with $N=6$ and $n_h=2$.

$V<V^*$, the modes qualitatively follow the AFM magnon dispersion $\bar{\omega}(q)=J|\sin(qa_0)|$ with values somewhat enhanced over the random-phase-approximation result. Again, the minimum frequency $\bar{\omega}(q)$ moves from $q_m=\pi/a_0$ to values $q_m\neq\pi/a_0$ for $V>V^*$.

In the limit $q\rightarrow 0$, the optical conductivity as defined by Eq. (8) is relevant to the optical absorption and reflectance measurements. For $N=6$ the lowest nonzero $q=\pi/3a_0$ is used for the analysis. For illustration we present in Fig. 5 a typical behavior of the integrated conductivities, defined by

$$L(\omega)\equiv\frac{2N}{a_0e_0^2}\int_0^{\omega}\mathrm{Re}\sigma(q,\omega')d\omega', \tag{14}$$

as they evolve for $n_h=2$ and $J/t=0.5$ with the increasing coupling V. From the sum rule, Eq. (10), we expect and find $(\omega\rightarrow\infty)=-E_{\mathrm{kin}}$. In all cases considered $L(\omega)$ reveals a pronounced two-step structure, which emerges from a single step at $V=0$. Note that since there are only two holes in the system, the absorption spectra at $V=0$ would show, for a given q, a *single* line at

$$\omega=\Delta\varepsilon_q=\varepsilon_q-\varepsilon_0=2t[1-\cos(qa_0)].$$

Hence, for $N=6$ with the lowest allowed $q=\pi/3a_0$, we have $\omega=t$. This simple structure for the bare holes clearly splits, for $V\neq 0$, into the two frequency regimes shown in Fig. 5.

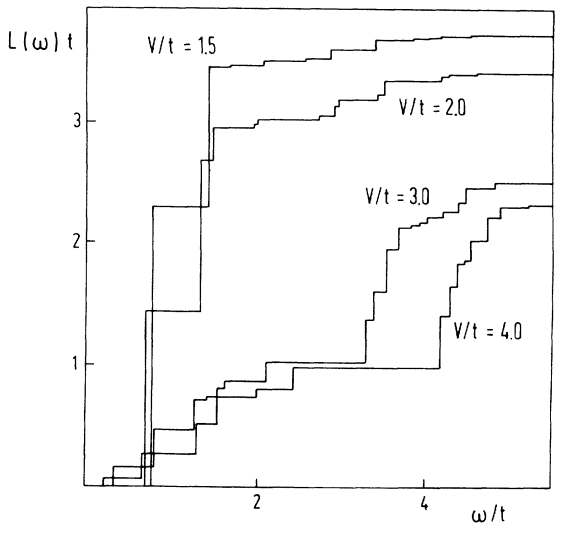

FIG. 5. Integrated optical conductivity $L(\omega)$ of a ring with $J/t=0.5$ and $N=6$, $n_h=2$. Results are for the lowest nonzero $q=\pi/3a_0$.

The step at lower ω, broadened for larger V/t, can be interpreted as the absorption of mobile quasiparticles. This part is also *expected* to merge into the Drude peak that would be present for $q\rightarrow 0$ in a larger system. Support for this expectation comes from the observations that in $\sigma(q=0,\omega)$ only the low-ω part is missing from the response, while the higher-ω behavior remains nearly unaffected. Importantly, one must recognize that our use of the terminology "Drude peak" is simply to be consistent with the colloquial usage in this area. In particular, since our (small) system size is possibly smaller than the mean free path of the quasiparticle, we are unable to make a meaningful frequency analysis of this regime. Specifically, we cannot estimate the relaxation time, τ, although some relaxation effects can already be resolved in the spectra for $\omega<\omega_c$, when $V>V^*$. From $L(\omega)$ we can extract the effective mass m^{**} of holes, enhanced over the band mass m^* due to interactions with spin fluctuations. Since the quasiparticle line at $\Delta\varepsilon_q$ is shifted to lower frequencies, one possible definition of the mass enhancement, $\tilde{\mu}_1=m^{**}/m^*$, would be $\tilde{\mu}_1=\Delta\varepsilon_q^0/\Delta\varepsilon_q$. It is, however, evident from Fig. 5 that due to the broadened quasiparticle absorption spectra this evaluation is not meaningful at $V>V^*$. Clearer is the division into the low-ω response of mobile quasiparticles and the higher-ω absorption related to internal quasiparticle excitations. This separation defines an enhancement $\tilde{\mu}_2$ through the sum rule $L(\omega_c)/L(\infty)=1-1/\tilde{\mu}_2$, where the cutoff ω_c is chosen in the plateau region $\omega_c>\Delta\varepsilon_q$. $1/\tilde{\mu}_2$ can be in this case interpreted as the weight of the Drude peak in the total optical absorption. The remaining absorption appears at much higher frequencies $\omega=\varepsilon_b\propto V$, where ε_b is the measure of the binding energy of the quasiparticle (magnetic polaron). As yet another indication of the enhanced mass one can use the reduced ground-state kinetic energy, $\tilde{\mu}_3=E_{\mathrm{kin}}(V)/E_{\mathrm{kin}}(V=0)$, where for $n_h=2$, $E_{\mathrm{kin}}(V=0)=-4t$.

Results for the various mass enhancements are presented in Fig. 6. The emphasis is on the sum-rule mass $\tilde{\mu}_2$ which shows a substantial increase for $V\lesssim V^*(J)$. The variation $\tilde{\mu}_2$ is approximately quadratic for small V. It can be described within the perturbation theory, as used in Ref. 10, which modified to the $d=1$ case yields $\tilde{\mu}_2=1+V^2/8\pi J^2$. Note that the dependence on J is predicted to be stronger here than in the $d=2$ case; this is indeed seen from the difference between the $J/t=0.1$ and 0.5 results. Again, the perturbation result for $d=1$ is only qualitatively correct, due to the absence of the long-range order.

Beyond $V^*(J)$ the enhancement decreases, approaching in the large-V limit the value $\tilde{\mu}_2=2$ for the mass of the

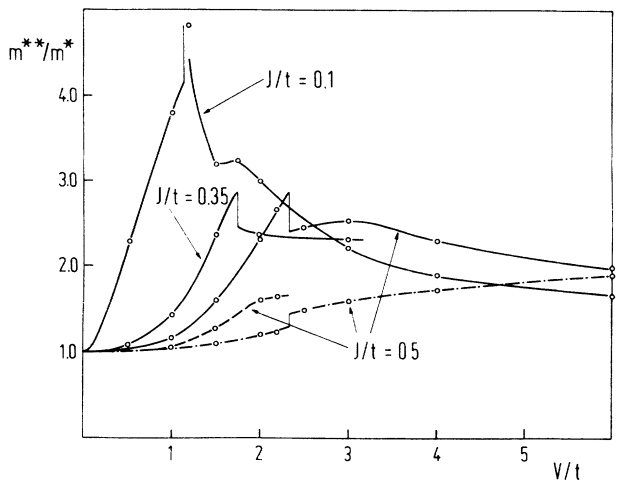

FIG. 6. Effective-mass enhancements $\tilde{\mu}=m^{**}/m^{*}$ of V/t for a ring. Full curves denote the sum-rule mass $\tilde{\mu}_2$, while dashed and dash-dotted curves show $\tilde{\mu}_1$ and $\tilde{\mu}_3$ behavior, as defined in the text.

bound singlets. The singlets are thus quite mobile entities, since their effective hopping matrix element is reduced only by $t_s \cong t/2$ with respect to the single-hole hopping. In particular, within the coupled-spin–mobile-hole model we would expect a clear Drude peak; this is as observed in the single-crystal samples of Y-Ba-Cu-O.[18] In Fig. 6 we present also the results for the two other measures of the effective mass, $\tilde{\mu}_1$ and $\tilde{\mu}_3$. $\tilde{\mu}_1$ shows a similar, but smaller increase at $V<V^{*}$, while the kinetic-energy reduction $\tilde{\mu}_3$ interpolates very smoothly between the two limits, i.e., $\tilde{\mu}_3=1$ at $V=0$ and $\tilde{\mu}_3=2$ at $V\rightarrow\infty$.

As far as the SC pairing is concerned, our results do not indicate a constructive role of the coupling V in the $d=1$ model. As discussed earlier, density correlations g_{ij} for $V>V^{*}$ are consistent with a pronounced *repulsion* between holes. At the same time, pairing correlations Z_{ss} and $Z_{s^{*},s^{*}}$, as defined by Eqs. (11) and (12) are clearly suppressed by finite V, especially for $V>V^{*}$; the effect is much stronger on Z_{ss}. Z_{pp}, which vanishes for $V=0$, increases slightly for $V>0$, but remains small, e.g., $Z_{pp}<0.05$ for $V/t<3$ and $J/t=0.1$.

For purposes of comparison, we have also performed numerical analysis of the initial model (1) on rings. In $d=1$ this model does not require a larger number of basis states; it merely involves additional terms in the Hamiltonian—e.g., for $V_2\neq 0$ we add to the $\mathbf{S}_i\cdot\mathbf{s}_i$ term also a $\mathbf{S}_{i+1}\cdot\mathbf{s}_i$ term assuming that O site i is between Cu sites i and $i+1$. We have diagonalized systems with $V_2>0$, $V_1=0$ and $V_1>0$, $V_2=0$. We will not discuss these results in great detail since they generally show the behavior observed for the simplified model (3). In particular, upon increasing the coupling in both cases $V_1=0$ and $V_2=0$, we find a rather abrupt change from the state with AFM correlations to a state where the maximum of $C(q)$ is at $q<\pi/a_0$. Also, local correlations $\zeta_{+}=-\sum_i\langle\mathbf{S}_i\cdot\mathbf{s}_i\rangle/n_h$, being equal to $\zeta_{-}=-\sum_i\langle\mathbf{S}_{i+1}\cdot\mathbf{s}_i\rangle/n_h$ in the $q_0=0$ ground state, show qualitatively the same behavior as in Fig. 2. However, the limiting value for large couplings is smaller than $\zeta=\frac{3}{4}$ allowed for in the model (3). In the large-V_2 limit, a localized $\mathbf{s}_i$ spin forms a $S_{\rm tot}=\frac{1}{2}$ state with neighboring $\mathbf{S}_i$ and $\mathbf{S}_{i+1}$ spins, where $\zeta_{-}=\zeta_{+}=\frac{1}{2}$. The situation in the $V_1\rightarrow\infty$ is more involved, since here the hopping is essential and the formation of the singlet is nonlocal.

The optical conductivity spectra were studied also in the presence of a V_2 term, and the results for the masses are similar to those given in Fig. 6. The calculation would be different for the V_1 term, since it would require a redefinition of the current operator (9) due to nonlocal hole scattering.

IV. VARIATIONAL APPROACH

A single mobile hole within the AFM state was studied in our previous paper[10] using a perturbation expansion in V. The validity of the latter is expected to break down for $V\gg t$, where local singlets composed of localized spins and mobile-hole spins form. In order to describe analytically the properties of a single hole (or low concentration of holes) in model (3) in the intermediate-coupling regime, we modify the variational approach[19] applied previously to the magnetic polaron problem.[20]

In traditional variational theories,[19,20] which become exact in the classical spin limit $S\rightarrow\infty$ for localized spins, the ansatz for a single fermion in the environment of localized spins is chosen to be

$$|\psi_0\rangle=\sum_i a_i\tilde{c}_{i\uparrow}^{\dagger}|0\rangle\prod_j|\tilde{\phi}_{j\downarrow}\rangle, \tag{15}$$

where both the hole operator $\tilde{c}_{i\uparrow}^{\dagger}$ and the local spin state $|\tilde{\phi}_{i\downarrow}\rangle$ refer, in general, to different *local* spin axes given by the angles φ_i and θ_i, i.e.,

$$\begin{aligned}\tilde{c}_{i\uparrow}^{\dagger}&=\cos\frac{\varphi_i}{2}c_{i\uparrow}^{\dagger}+\sin\frac{\varphi_i}{2}c_{i\downarrow}^{\dagger},\\ |\tilde{\phi}_{i\downarrow}\rangle&=\cos\frac{\theta_i}{2}|i\uparrow\rangle+\sin\frac{\theta_i}{2}|i\downarrow\rangle,\end{aligned} \tag{16}$$

and $\sum_i a_i^2=1$. Since the ansatz (15) does not allow for a formation of a local singlet out of $\mathbf{s}_i\cdot\mathbf{S}_i$, which we have argued is crucial for $S=\frac{1}{2}$, we supplement Eq. (15) by allowing configurations with locally flipped spins,

$$|\psi\rangle=\sum_i a_i(\cos\nu_i\tilde{c}_{i\uparrow}^{\dagger}+\sin\nu_i\tilde{c}_{i\downarrow}^{\dagger}\tilde{S}_i^{+})|0\rangle\prod_j|\tilde{\phi}_{j\downarrow}\rangle, \tag{17}$$

where $\tilde{S}_i^{+}$ flips the localized spin on site, i.e.,

$$S_i^{+}|\tilde{\phi}_{i\downarrow}\rangle=|\tilde{\phi}_{i\uparrow}\rangle=\sin\frac{\theta_i}{2}|i\uparrow\rangle+\cos\frac{\theta_i}{2}|i\downarrow\rangle. \tag{18}$$

Note that Eq. (17) reproduces both limits—the unperturbed hole motion with $\nu_i=0$ and the local singlet formation with $\nu_i=-\pi/4$—correctly. With the ansatz (17) we find the energy to be

$$\begin{aligned}E=&-t\sum_{\langle i,j\rangle}a_i a_j\cos\nu_i\cos\nu_j\cos\frac{\varphi_i-\varphi_j}{2}\\&+\frac{V}{4}\sum_i a_i^2[\cos(\theta_i-\varphi_i)(1+\sin2\nu_i)-\sin2\nu_i]\\&+\frac{J}{4}\sum_{\langle i,j\rangle}\cos(\theta_i-\theta_j)[1-2(a_i^2\sin^2\nu_i+a_j^2\sin^2\nu_j)].\end{aligned} \tag{19}$$

The expression (19) is identical to that of Umehara and Kasuya[20] when $v_i=0$. Solutions for a_i, v_i, φ_i, θ_i can be found through the minimization of E.

In general, Eqs. (19) have to solved numerically. The problem can be greatly simplified, however, by noting that a delocalization function, i.e., $a_i=\tilde{a}_i/\sqrt{N}$, represents one of the solutions. The θ_i, following the AFM order, then alternate between the values 0 and π; also, we can choose $\varphi_i=0$. $\tilde{a}_i$ and v_i then have only two values: namely, $\tilde{a}_1,\tilde{a}_2=(2-\tilde{a}_1^2)^{1/2}$ and $v_1=0$, while $v_2=0$ on sites with $\varphi_2=\theta_2$. Thus the problem reduces to two coupled equations for $\tilde{a}_1$ and v_1:

$$2\sin v_1(2t\tilde{a}_2+J\tilde{a}_1\cos v_1)=V\tilde{a}_1\cos 2v_1\,, \tag{20}$$

$$2t\cos v_1(\tilde{a}_1-1)=\tilde{a}_1\tilde{a}_2[V(1+\sin 2v_1)+J\cos^2 v_1]\,. \tag{21}$$

These equations indicate a linear dependence $v_1\propto V$ at small V. The result for ζ, following from Eqs. (19)–(21), is also presented in Fig. 2. It is only weakly dependent on J/t and is seen to represent numerical values at $V<V^*$ quite well. Note that spin correlations in this state are still of the AFM type.

Although Eqs. (20) and (21) reproduce the singlet state in the $V\to\infty$ limit, the lowest-energy solution of Eq. (19) in this regime does not correspond to a delocalized hole in an AFM ordered environment. The solution is rather a localized hole within a locally distorted configuration of spins $\mathbf{S}_i$. We restrict ourselves here to a rather crude analysis of this case. We assume that within a chain there is a region (of length N_l) of spins $\mathbf{S}_i$ with a predominantly FM correlation, i.e., $\theta_i=0$, $i=1,N_l$. In the same way we simplify Eq. (19) by taking $a_i=1/\sqrt{N_l}$, $v_i=v$, and $a_i=0$ outside this region. Since in this case also $\varphi_i=0$, the energy of a localized hole can be written as

$$\Delta E=-2\alpha t\cos^2 v-\frac{V}{4}(1-2\sin 2v)+N_l\alpha\frac{J}{2}-J\alpha\sin^2 v\,, \tag{22}$$

with $\alpha=1-1/N_l$, so that finally $v=-V/\alpha(2t-J)$. As is also indicated in Fig. 2(a), for larger V, the localized state shows a larger correlation ζ than a delocalized one. It also accounts properly for the behavior above the transition $V>V^*$. In the case $J/t=0.1$, the minimum of ΔE is obtained for $N_l=5$, while it reduces to $N_l=3$ for $J/t=0.5$. An estimate of the transition point V^*, obtained by comparing the energies of localized an delocalized solutions, is less satisfactory, e.g., at $J/t=0.1$ we get $V^*/t=1.9$ while the numerical results give $V^*/t=1.15$. The latter state is consistent with the observation that above V^* short-range AFM correlations are greatly reduced or even turn to weakly FM ones. It should be stressed, however, that the main effect for $V>V^*$ is a nearly complete formation of a local singlet with $\zeta=\frac{3}{4}$. A description of the magnetic polaron (with $S=\frac{1}{2}$ spins) only in terms of a classical spin ansatz (15) would be thus quite inappropriate. In $V>V^*$ regime there is also a substantial similarity with the concept of mobile holes within the single-band Hubbard model, as discussed in Refs. 1–4.

Finally, we note that the clear semiquantitative agreement of this (large system) variational approach with our (small system) exact diagonalization studies of the properties of *single* holes provides strong evidence that, despite our limited range, finite-system-size effects are *not* distorting our conclusions for these properties.

V. NUMERICAL RESULTS FOR A SQUARE LATTICE

We study model (3) numerically also on a small system of $N=2\times3=6$ sites, embedded in a square lattice. In order to allow for a AFM order we require staggered boundary conditions, as shown in Fig. 7. For the model (3) numerical requirements are the same as for a system on a ring; in contrast the model defined by (1) and (2) would need a much larger Hilbert space in $d=2$. We do not attempt to compute the optical conductivity, since the linear dimensions are too small for a reasonable extrapolation of results $\sigma(\mathbf{q},\omega)$ to $\mathbf{q}\to 0$.

In Fig. 8 results for ζ on a square lattice are presented. The linear increase at small V and the saturation at large V are similar to results observed on a ring. In the intermediate regime, however, ζ shows a *gradual* increase, as opposed to a *discontinuous* one in $d=1$. Still, a region of a qualitative change in ζ and other quantities can be located, e.g., $V^*/t\sim1.7$ at $J/t=0.1$ and $V^*/t\sim2.3$ at $J/t=0.3$. The discontinuity at $V>V^*\sim3t$ for the $J/t=0.3$ case is due to the instability against $\mathbf{q}_0\neq0$ state and seems not to be indicative of the general qualitative behavior.

Similar conclusions follow from susceptibilities $\chi(\mathbf{q})$ and frequency moments $\bar{\omega}(\mathbf{q})$, as drawn in Figs. 9 and 10. Note that for given boundary conditions we can define three inequivalent $\mathbf{q}$, i.e., $\mathbf{q}_1=\pi(1,1)/a_0$ corresponding to AFM ordering, $\mathbf{q}_2=\pi(\frac{1}{3},1)/a_0$, and $\mathbf{q}_3=\pi(\frac{2}{3},0)/a_0$. For all J/t there is a clear maximum in $\chi(\mathbf{q}_1)$ at small V. AFM correlations gradually disappear at $V\sim V^*(J)$.

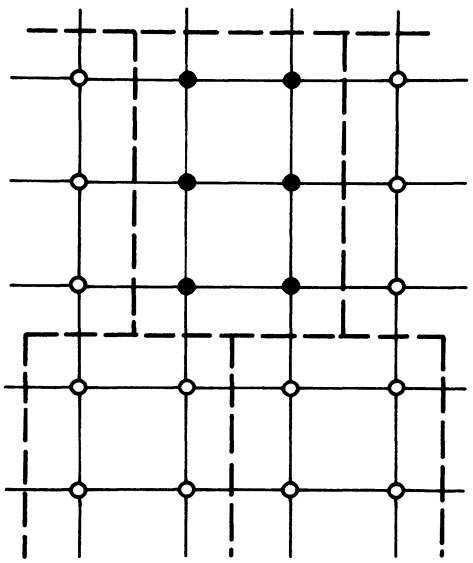

FIG. 7. Boundary conditions used for a $N=6$ system, embedded in the square lattice.

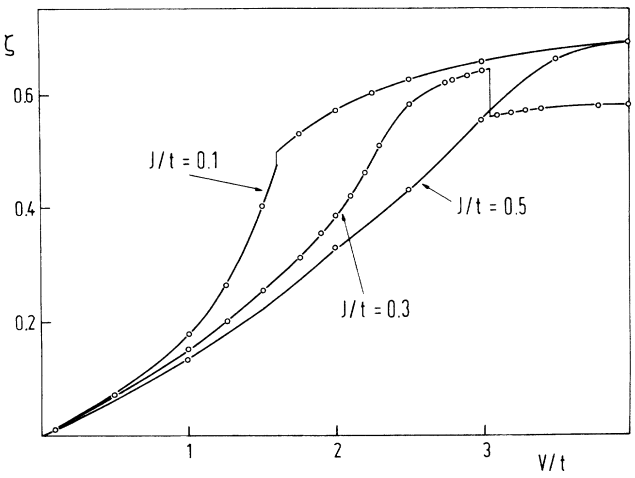

FIG. 8. Local spin correlation function ζ for a square lattice with $N=6$ and $n_h=2$.

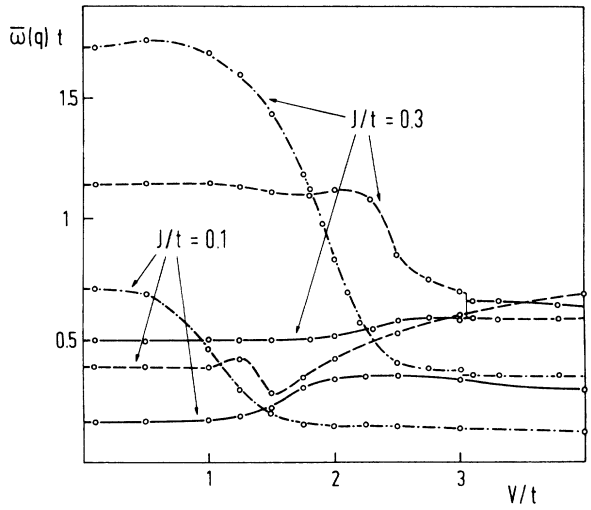

FIG. 10. Spin-fluctuation frequency moments $\bar{\omega}(q)$ for a square lattice with $N=6$ and $n_h=2$.

The continuous change is clearly evident in the softening of highest-frequency modes in Fig. 10. Beyond V^*, $\chi(\mathbf{q})$ exhibits only a weak $\mathbf{q}$ dependence (for $J/t=0.3$ and 0.5 cases) with a slight dominance of $\mathbf{q}_1$ and $\mathbf{q}_3$ values. For $J/t=0.1$ the smallest $\mathbf{q}_3$ dominates, indicating a tendency toward a short-range FM ordering. The results for $\bar{\omega}(\mathbf{q})$ qualitatively follow the expected AFM magnon dispersion at $V<V^*$. Moreover, they show that also for $V>V^*$ the frequency range is determined by J, i.e., $\bar{\omega}(\mathbf{q})\propto J$, and not by much larger V. Thus, the spin dynamics seem to be dominated still by localized spins and their interactions.

For a square lattice, in addition to Δ_s and Δ_p, as defined in Eqs. (12), we study also s^*- and d-wave SC pairing operators,

$$\Delta_{s^*}=2\sum_{\langle i,j\rangle}c_{i\uparrow}c_{j\downarrow},\quad \Delta_d=2\sum_{\langle i,j\rangle}(-1)^{x_{ij}}c_{i\uparrow}c_{j\downarrow}, \tag{23}$$

where $\langle i,j\rangle$ are nearest-neighbor O sites and $x_{ij}=\mathbf{R}_{ij}\cdot\mathbf{e}_x/a_0$. The results for Z_{ss}, $Z_{s^*s^*}$, and Z_{dd} are presented in Fig. 11. The s-wave pairing is strongly suppressed for finite V, especially for $V>V^*$. The decrease of $Z_{s^*s^*}$ with V is weaker. Z_{pp} is negligible in the whole regime. On the other hand, Z_{dd} increases with V, although it remains small for all V. The starting $Z_{dd}(V=0)=0$ stems from the fact, that for $n_h=2$ both holes are in the ground state with a well defined wave vector $\mathbf{k}=0$. Ignoring the discontinuity due to the appearance of a degenerate state for $J/t=0.3$, our results *could* be an indication for a SC d-wave pairing. This interpretation should be taken with care since Z_{dd} is still small, in fact not larger than $Z_{s^*s^*}$, and may be also enhanced due to our use of a nonsymmetric 3×2 cluster.

There is, however, an essential difference between $d=1$ and $d=2$ systems for $V>V^*$. Whereas on a ring the density correlations reveal a repulsion between holes,

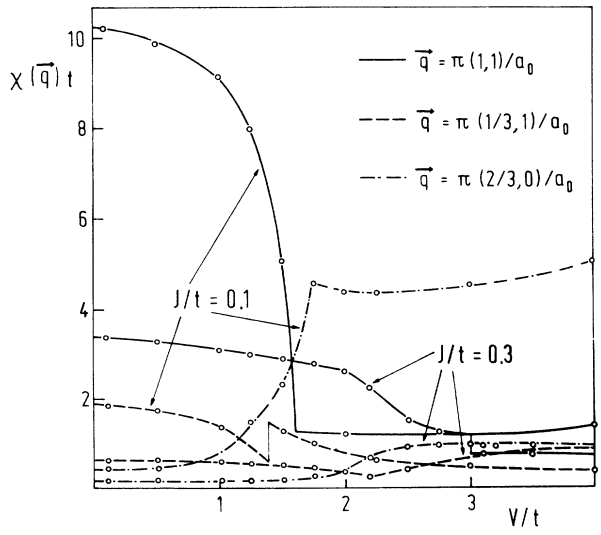

FIG. 9. Susceptibility $\chi(\mathbf{q})$ as a function of V/t for a square lattice with $N=6$ and $n_h=2$.

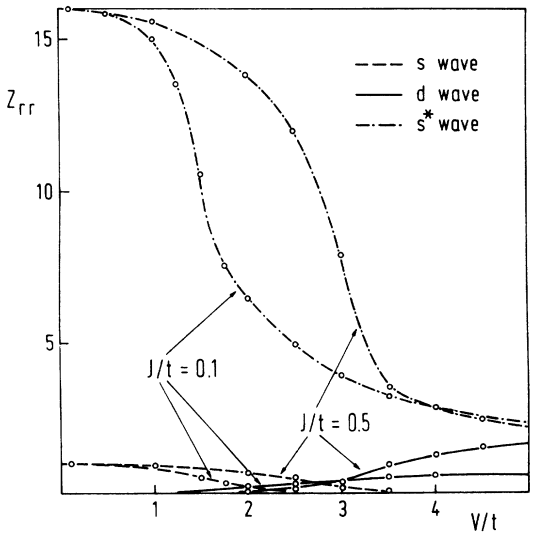

FIG. 11. Pairing correlations Z_{rr} for $r=s$-, d-, and s^*-wave functions, respectively, on a square lattice.

there is no such effect on a square lattice. Specifically, g_{ij} is nearly constant for $i \neq j$, although we observe a weak decrease in g_{ij} for neighboring ij. This result provides an indication against a real-space pairing, but it would possibly allow an attractive interaction in the $\mathbf{k}$ space in the presence of a Fermi sea of holes.[4] In this regard, it is important to stress that for superconducting pairing properties, finite-size effects may influence our results substantially. This is in contrast to the situation for the single-hole properties of our model, where by similarity of both the $N=4$ and 6 results with the conclusions of the variational ansatz, finite system effects could be shown to be negligible.

VI. CONCLUSIONS

In this paper we have treated a model, potentially relevant to the SC copper oxides, involving a coupled system of localized spins and mobile holes. Exact numerical diagonalizations of small systems, performed at a fixed number of mobile holes $n_h=1,2$, show as a function of the coupling strength V a transition from a regime of weakly perturbed hole motion to the regime of mobile local singlets. The latter are formed locally out of localized Cu spins and mobile holes, mainly on O sites. The internal structure of a singlet depends on details of the particular model; in particular, the results are somewhat different for models (1) and (3). In contrast, the general properties of the system are expected to be more universal. Our results for a square lattice ($d=2$) indicate a rather continuous, soft-mode-like transition between the two regimes, while on the $d=1$ ring the transition is more abrupt. The transition at $V \sim V^*$ is also connected with qualitative changes in most relevant quantities. Whereas for $V < V^*$, total spin correlations show at least a short-range AFM order, AFM correlations are reduced or even become FM above the transition, depending on the parameter J/t.

Clearly, the understanding of a single hole in the perturbed AFM environment is crucial for a description of the above results. We denote this entity still as the "magnetic polaron," although as noted above it is far from the conventional classical spin ansatz, Eq. (16). In the intermediate (or strong) V regime, it is in fact much closer to a concept of local singlets[11] or even resonating-valence-band droplets.[22]

A very important quantity for comparison with experiments is the optical conductivity of the magnetic polarons. The effective hole mass m^{**}, defined by a low-frequency sum rule relevant to optical-absorption experiments, is shown (for the $d=1$ ring) to *increase* with the coupling at small V. Moreover, it goes through a *maximum* at $V \sim V^*$ and then decreases to the value appropriate for the singlets, where the mass enhancement is $\tilde{\mu}_2 = m^{**}/m^* \approx 2$. Our results do not support the large enhancements $\tilde{\mu}_2 > 5$, such as were used in Ref. 17 to interpret the optical conductivity results on ceramic samples.[13–15] Rather, we find modest enhancements which are consistent with the recent measurements on single crystals of Y-Ba-Cu-O.[18]

With respect to SC pairing our results are less conclusive. They give no indications for a formation of real-space hole pairs, which should show up, for example, in hole-density correlations. Moreover, in the $d=1$ ring, strong hole-hole repulsion is evident for $V > V^*$, leading to hole ordering at distances $L_0 = N/n_h$. On a square lattice there is no evidence for a repulsion between holes if they are more distant than nearest neighbors. For the same reasons, the SC pair correlations Z_{rr} are either small or suppressed by finite coupling V. In the intermediate V regime s-wave pairing is reduced much more strongly than s^*-wave pairing, while d-wave pair correlations increase with V. Still Z_{dd} remains small, even smaller than $Z_{s^*s^*}$ in the whole V regime, so that our evidence in favor of d- or s-wave pairing should be taken with care.

On a more phenomenological level, we can argue that for larger doping the mobile holes (or quasiparticles) interact via spin fluctuations, which are mainly due to localized spins on Cu sites. This concept seems to remain reasonable even for larger V, since the paramagnon frequencies $\bar{\omega}(\mathbf{q})$ are still governed by $J \ll t$, and not by the much larger V. In a phenomenological theory the static susceptibility $\chi(\mathbf{q})$ serves as input; an example is the analysis of heavy fermion SC.[23] In a weak-coupling regime we have shown[10] that in an ordered AFM state magnons do not lead to a constructive pairing in any of the s-, p-, or d-wave channels. However, our numerical results show that beyond $V > V^*$, $\chi(\mathbf{q})$ changes in an essential manner with the maximum moving away from $q = q_{\mathrm{AFM}}$. This could allow for an attractive interaction, leading to a d-wave pairing, or possibly even s^*-wave pairing

ACKNOWLEDGMENT

This work was supported by the U.S. Department of Energy.

*Permanent address: Department of Physics and J. Stefan Institute, E. Kardelj University of Ljubljana, 61000 Ljubljana, Yugoslavia.

[1] P. W. Anderson, Science **235**, 1196 (1987).
[2] G. Baskaran, Z. Zou, and P. W. Anderson, Solid State Commun. **63**, 973 (1987); P. W. Anderson, G. Baskaran, Z. Zou, and T. Hsu, Phys. Rev. Lett. **58**, 2790 (1987).
[3] A. Ruckenstein, P. J. Hirschfeld, and J. Appel, Phys. Rev. B **36**, 857 (1987).
[4] C. Gros, R. Joynt, and T. M. Rice, Z. Phys. B **68**, 425 (1987).
[5] J. E. Hirsch and H. Q. Lin, Phys. Rev. B **37**, 5070 (1988).
[6] H. Q. Lin, J. E. Hirsch, and D. J. Scalapino, Phys. Rev. B **37**, 7359 (1988).
[7] V. J. Emery, Phys. Rev. Lett. **58**, 2794 (1987).
[8] J. E. Hirsch, Phys. Rev. Lett. **59**, 228 (1987).
[9] M. Imada, J. Phys. Soc. Jpn. **56**, 3793 (1987).
[10] P. Prelovsek, Phys. Lett. A **126**, 287 (1988).
[11] F. C. Zhang and T. M. Rice, Phys. Rev. B **37**, 3759 (1988).
[12] J. M. Tranquada, S. M. Heald, A. R. Moodenbough, and M. Suenaga, Phys. Rev. B **35**, 7187 (1987); A. Fujimori, A. Takayama-Muromachi, and Y. Uchida, Solid State Commun. **63**, 857 (1987).

[13]J. Orenstein, G. A. Thomas, D. H. Rapkine, C. G. Bethea, B. F. Levine, R. J. Cava, E. A. Rietman, and D. W. Johnson, Jr., Phys. Rev. B **36**, 729 (1987).

[14]K. Kamaras, C. D. Porter, M. G. Doss, S. L. Herr, D. B. Tanner, D. A. Bonn, J. E. Greedan, A. H. O'Reilly, C. V. Stager, and T. Tikmusk, Phys. Rev. B **36**, 733 (1987).

[15]S. Etemad, D. E. Aspnes, M. K. Kelly, R. Thompson, J.-M. Tarascon, and G. W. Hull, Phys. Rev. B **37**, 3396 (1988).

[16]C. M. Varma, S. Schmitt-Rink, and Elihu Abrahams, Solid State Commun. **62**, 681 (1987).

[17]R. B. Laughlin and C. B. Hanna (unpublished); D. J. Scalapino, R. T. Scalettar, and N. E. Bickers, in *Novel Superconductivity,* edited by S. A. Wolf and V. Z. Krezin (Plenum, New York, 1987).

[18]Z. Schlesinger, R. T. Collins, D. L. Kaiser, and F. Holtzberg, Phys. Rev. Lett. **59**, 1958 (1987).

[19]P. G. de Gennes, Phys. Rev. **118**, 141 (1960).

[20]M. Umehara and T. Kasuya, J. Phys. Soc. Jpn. **33**, 602 (1972).

[21]G. Shirane, Y. Endoh, R. J. Birgeneau, M. A. Kastner, Y. Hikada, M. Oda, M. Suzuki, and T. Murakami, Phys. Rev. Lett. **59**, 1613 (1987).

[22]T. K. Lee, C. Zhang, and L. N. Chang (unpublished).

[23]K. Miyake, S. Schmitt-Rink, and C. M. Varma, Phys. Rev. B **34**, 6554 (1986).